



Adaptive 6 DOF Self-Balancing Platform for Autonomous Vehicles

Mohammad Alkhedher¹, Tariq Younes², Omar Mohamad³ and Uzair Ali⁴

^{1,3,4} Mechanical Engineering Department, Abu Dhabi University, Abu Dhabi, United Arab Emirates

² Mechatronics Engineering Department, Al Balqa Applied University, Amman, Jordan

Received 17 Jul. 2019, Revised 20 Dec. 2019, Accepted 30 Dec. 2019, Published 01 Jan. 2020

Abstract: Parallel manipulators with six degrees of freedom are utilized in many applications. In this paper, a Stewart manipulator is used as a robust vehicle stabilizer to control the orientation and direction of the top platform. A detailed kinematic analysis of a Stewart platform is established in order to control the extensions of linear actuators. This analysis is formulated to cope with the design of vehicle stabilizer. The design and selection of mechanical components including primary joints is accomplished based on comprehensive dynamic simulation. After validating simulation results of proposed design, they were implemented in to build a physical model. To improve system accuracy and performance, and to eliminate associated vibrations, a linear regression model of ground rise is embedded in the system to estimate and predict upcoming elevations. This has lowered the percentage error of platform orientation, made the system more stable.

Keywords: Stewart platform, Kinematics, Simulation, stabilizer, Linear regression

1. INTRODUCTION

Parallel mechanisms with 6 Six Degree of Freedom (6 DOF) Platforms have many applications worldwide. The parallel kinematic structure of Stewart platforms is used to control motion in 6 DOF in applications as manufacturing processes and precise manipulative tasks. The Stewart platform structure offers better performance than serial structure, it possess higher precision and higher power-to-weight-ratio [1, 2]. The construction of Stewart platform manipulators is profoundly discussed in literature [3, 4].

It is well-known that 6 DOF platforms are accurate, fast, and precise [5]. Also, the workspace is large enough to accommodate any practical path, as the top platform can rotate with angles exceeding 45° relative to the base. Several designs of 6 DOF platforms were introduced by researchers to service different applications as flight simulators. For example Atlas Flight Simulator is introduced Carleton University [6]. A kinematic design of a 6-DOF parallel manipulator with decoupled translation and rotation is discussed in [7].

Another innovative design is 6-DOF triple scissor extender robots with applications in aircraft assembly [8] with 6 limbs where each limb consists of several links that are connected with revolute joints. Design of a 6-DOF robotic platform for wind tunnel tests of floating wind

turbines is developed to test floating offshore wind turbines in a wind tunnel [9].

Recently application of six-degrees-of-freedom parallel mechanism in micro-positioning has been developed [10], the moving platform has a multiaxial spherical joint at its bottom side where three internal limbs are attached to it in a tetrahedron arrangement. Another three external limbs are connected to the platform directly. Other applications include dynamic control of micro-vibration simulator is proposed using 6-DOF platform for performance testing of sensitive instruments in a micro-vibration environment on-board spacecraft before launch. [11].

The objective of this research work is to utilize 6 DOF Stewart mechanism in stabilizing the upper platform for any vehicle facing variations in path bumpiness. An intelligent vehicle stabilizer using 6-DOF Stewart platform will be designed and constructed as a parallel mechanism that consists of a rigid body moving plate, connected to a fixed base plate through six independent kinematics legs. A Reference trajectory is generated based on the feedback sensing elements of each actuator based on inverse kinematic and inverse dynamic models, several control schemes are implemented to achieve highest performance of the controller and the system.

2. KINEMATIC ANALYSIS

Different algorithms are implemented to achieve accurate control of parallel manipulators. Most of these methods depends on inverse kinematics and inverse dynamics study [12]. An inverse kinematic model is derived to be used in controlling the motion of the platform to a desired position and direction. The control algorithm will give the orders to generate the required motion for each leg actuator in order to reach a desired position that is calculated based on inverse kinematics.

The inverse kinematic analysis of a 6-DOF parallel manipulator is modeled using vector loop method as shown in Figure 1. There are two frames describing the motion of the moving platform : first frame located in the center of base plate (X_B, Y_B, Z_B) which considered to be the reference frame work, the second one is located in the center of top plate (X_P, Y_P, Z_P). Positions of base and platform are uniquely defined by coordinates of the six joints that connect them with links [13, 14].

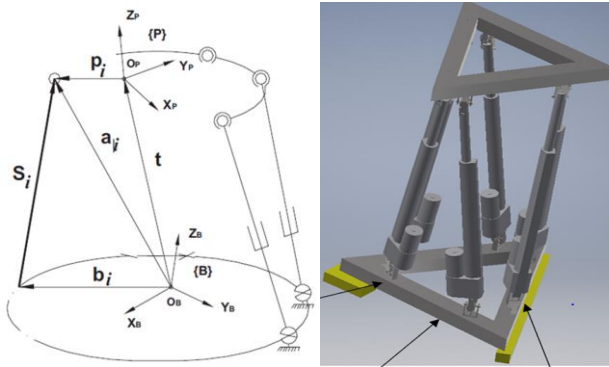


Figure 1. 6-DOF parallel manipulator vector loop.

The aim of inverse kinematics is to compute the desired length of each leg to control the motion of the platform. In Figure 1 (p_i and b_i) are joint positions in platform and base respectively, the lines that connect each one with the origin is called (position vector), in inverse kinematics the plate goes to the needed position as the required, so it is required to determine the needed movement of the plate, only (X_B, Y_B) reference plane is used, so the movement of the top plate will be illustrated with respect to the base, where the line (S_i) shows this relative motion, and (a_i) is the line that connect the origin of the base with the joint position (p_i). R_b is the radius of the lower base [15].

Defining the expected length of every linear actuator in Stewart platform, S_i , in the form:

$$S_i = R p_i + t - R_b b_i \quad (1)$$

$$R = R_z * R_y * R_x \quad (2)$$

$$R_z = \begin{bmatrix} \cos \theta_z & -\sin \theta_z & 0 \\ \sin \theta_z & \cos \theta_z & 0 \\ 0 & 0 & 1 \end{bmatrix} \quad (3)$$

$$R_y = \begin{bmatrix} \cos \theta_y & 0 & -\sin \theta_y \\ 0 & 1 & 0 \\ \sin \theta_y & 0 & \cos \theta_y \end{bmatrix} \quad (4)$$

$$R_x = \begin{bmatrix} 1 & 0 & 0 \\ 0 & \cos \theta_x & \sin \theta_x \\ 0 & -\sin \theta_x & \cos \theta_x \end{bmatrix} \quad (5)$$

Where R is the coordinate transformation matrix as defined in (2) and (3)-(5). p_i represents the upper joints coordinates reference to the center of upper platform. b_i are the lower joints coordinates reference to the center of lower platform. t is the relative distance between the centers of upper and lower platforms [16].

The Stewart platform assumes a fixed lower base and a free upper platform. However, a vehicle stabilizer assumes a free lower base while an ideally fixed upper platform in all degrees of freedom except along the rotation in the z axis. Thus, the inverse kinematic equation of the stabilizer would vary from the Stewart platform equation in terms of the location of the rotation matrix as shown in (6)-(7):

$$S_i = p_i + t - R b_i \quad (6)$$

$$R = R_y * R_x \quad (7)$$

3. MODEL SIMULATION

Prior validation of proposed design is achieved by modeling the inverted Stewart platform using Simscape Multibody package. The model is shown in Figure 2.

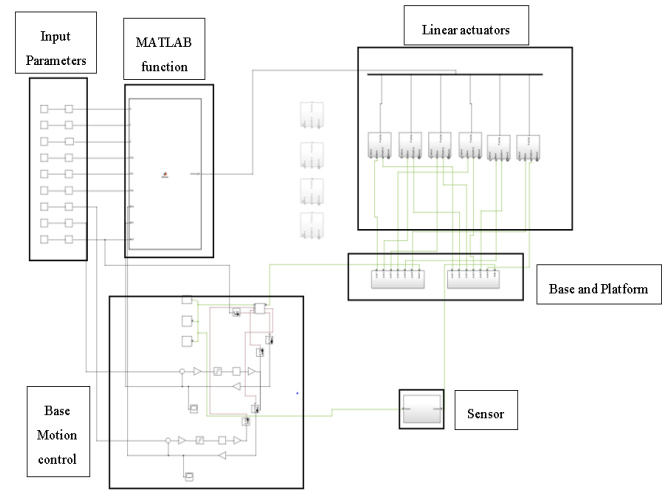


Figure 2. Simulated model of vehicle stabilizer

As shown above, in the second column of blocks are gain slider where the maximum and minimum values are adjusted, the translation in X , Y , and Z axes represent the values of the (t) vector which extends from the center of the stabilizer, these three values should remain constant with the X and Y being at zero and the Z being equal to the vertical distance between the platform and the base when

the length of each actuator is 15cm, this value is 67.5cm. The orientation of the top platform are set to zero since the aim of the stabilizer is to keep the platform at its position regardless of the position of the base. An IMU sensor is mounted on the base to measure all required inputs including orientations. The rotation of the base along the Z is excluded from this action as the stabilizer doesn't react when the mechanism rotates in the Z axis.

The function is fed with the input parameters which specify the required position of the platform with respect to the base, and the output of the function is the length of each actuator. Thus, it should be noted that the output is a six-element vector.

The input required position of linear actuators represents the stabilized position of the upper platform is compared with the current position of the linear actuator. The value obtained passes through the controller which is a PID controller. The saturation block limits the output value to only 10mm/s in either directions. This value represents the speed of the used linear actuator. The extension and position of linear actuators is then determined. The current position is also found using a position sensor. An example of one linear actuator is shown in Figure 3.

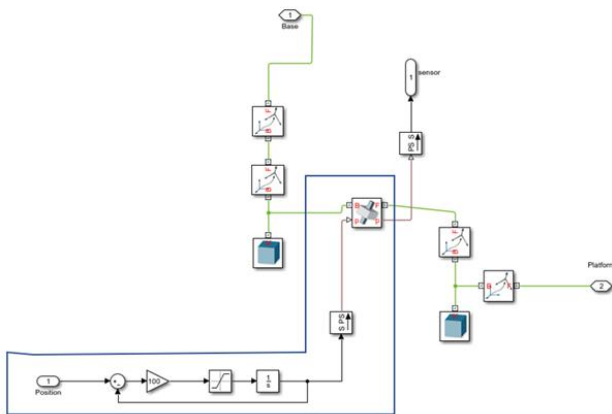


Figure 3. Controller of linear actuator

The base is connected to the reference axis through a gimbal joint which can rotate about any of the three axes (three angular degrees of freedom). The movement of this joint is completely controlled using the last three input parameters. For any angle chosen along the X or Y axis, the base will start rotating at a maximum speed of 20/s until it reaches the required angle. Every 4ms (250Hz), the position of the base is fed to the controller function to calculate the required position that each actuator should go. The angle of rotation about the Z axis is maintained at zero to prevent the base from rotating along the Z axis due to the movement of the actuator.

The controller used in the simulation was a proportional-derivative controller. A test case for the position of platform while base is rotating about the x-axis is shown in Figures 4 and 5. The percentage error was about 0.35%, 3.75%, and 0.2% in the x, y, and z axes, respectively.

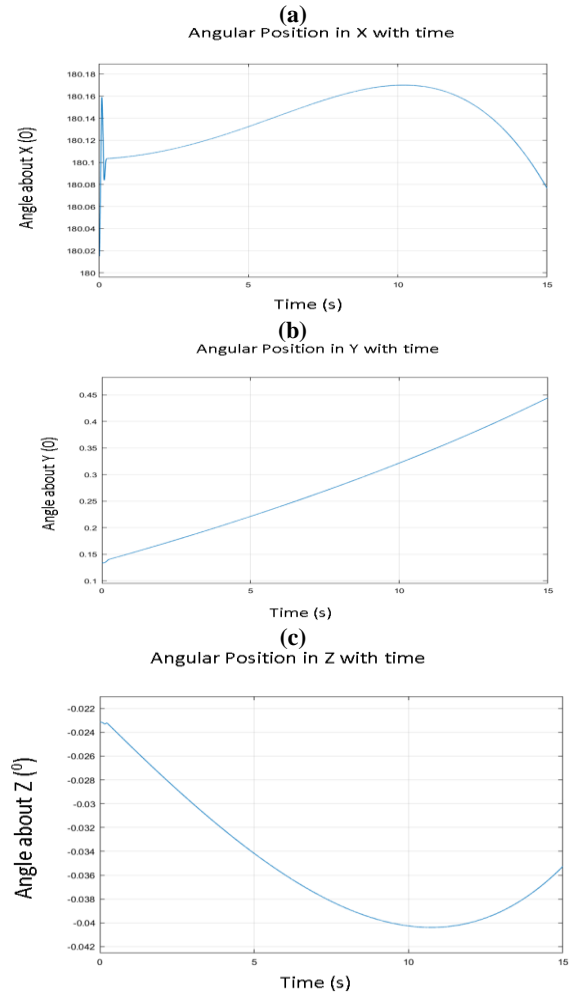


Figure 4. Translation and rotational movement of top platform with respect to the 3 axes respectively

As shown in Figure 5, the platform was capable of stabilizing itself as the base rotated from 0 to 30° at almost all points of time. As shown in movement of the platform along the X and Z axis is less than 1.5mm while on the Y axis it about 11mm. However, the platform is made from an equilateral triangle whose length is 40cm; thus, 1.1 cm will only lead an error of about 2.75% making it hardly visible to the vehicle user. The rotation of the platform along all the axes is less than 0.3° throughout the whole stabilizing process.

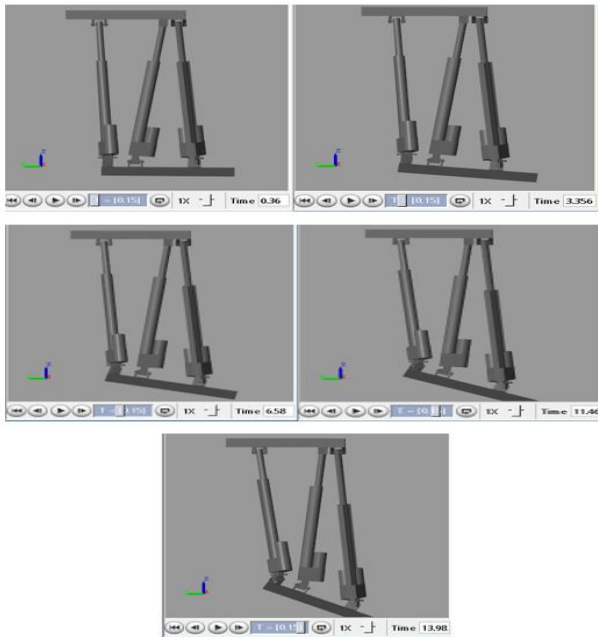


Figure 5. Position of top platform as the base rotates 30° about X axis

4. PHYSICAL PROTOTYPE

The main prototype consisted of six extendable legs (linear actuators) connected to the base and platform with universal joints as shown in Figure 6.



Figure 6. Final design of vehicle stabilizer

Each motor is connected to a full bridge motor driver that gets the signal from a microprocessor. Two 6-DOF inertial measurement unit (IMU) sensors are used. One of them is connected to the base while the other is connected to the top platform. The readings of the base sensor are fed to the microprocessor as the rotation matrix to find the required length of the linear actuators. A PD controller is used to ensure that each linear actuator reaches the required position.

The control implementation diagram is shown in Figure 7.

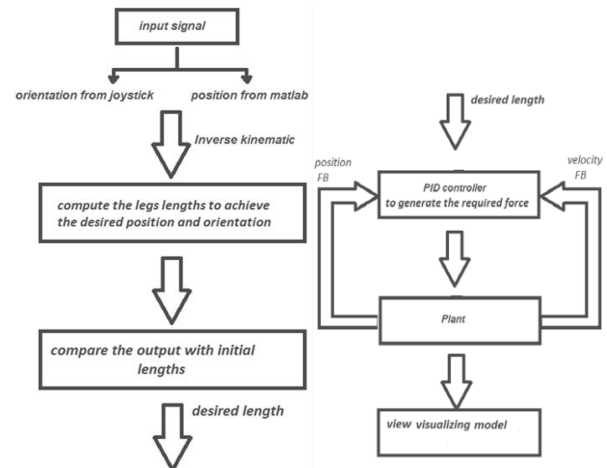


Figure 7. Flow Chart for designing a Stewart platform model.

Disregarding the yaw, the pitch and roll can be found either by using the accelerometer or the gyroscope. However, it is common to combine the two sensors in a single IMU unit such as the MPU 6050. This is used to compensate for the problems associated with every sensor. In the case of the accelerometer, vibrations will affect the readings making it susceptible to noise. On the other hand, gyroscopes suffer from drifting which is the change in readings with respect to time without a real change in position. Thus, combining the two results using a filter will yield more accurate results than using any of the sensors individually.

The filter used in this project is the complimentary filter. Using this filter, the pitch and roll can be found accordingly:

$$X = (X_{old} + \omega_x dt) * 0.98 + X_a * 0.02 \quad (8)$$

$$Y = (Y_{old} + \omega_y dt) * 0.98 + Y_a * 0.02 \quad (9)$$

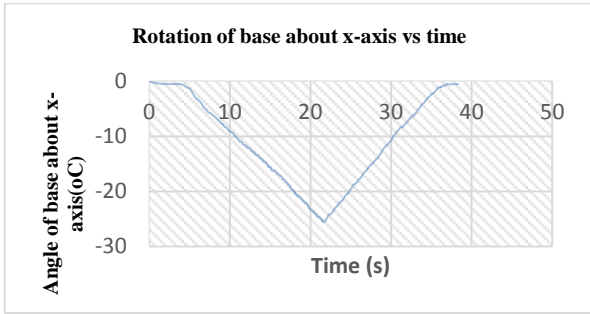
X_{old} and Y_{old} are the previous values of roll and pitch respectively, ω_x and ω_y are the angular velocities in the x and y direction respectively, X_a and Y_a are the roll and pitch found using the accelerometer readings respectively

The concept of this filter is to make the effect of the gyroscopic reading more significant decreasing the error caused by the accelerometer readings during noise. In the same time, when the object is stationary, the speed to the drift of the gyroscope will be small allowing the accelerometer reading to stabilize the reading and ensuring that the correct angle is reached. There are various other filters that can be used; however, they are more mathematically demanding.

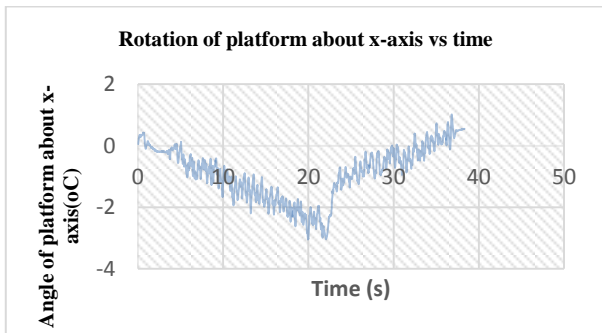
Figure 8(a) shows the input ramp signal due to a pathway bump. As shown in Figure 8(b), the maximum angle reached is about 3° (12%) even though the angle that the base is rotated about is 25°. The negative sign



comes from the orientation of the sensor. The top platform undergoes 1° vibration along the rotation. This results in an undesirable jerky behavior.



(a)



(b)

Figure 8. Rotation of (a) base and (b) platform w.r.t X-axis

5. LINEAR REGRESSION

In the previous stage, it was shown that the stabilizer only senses the rotation of the base after it rotates. However, it was suspected that this is leading to the jerky effect, so artificial intelligence was introduced into the system to predict the future position of the base before it rotates. Reference [17] suggested the use of dynamic neural network. Other work suggests optimal control of a Stewart robot using a sequential optimal feedback linearization method considering the jack dynamics to secure optimal and accurate control of a Stewart robot that is supposed to carry a machine along a specified path [18]

Other recent work proposed H-infinity theory to control 6 DOF motion [19]. However, to avoid complexity and high computation requirements, linear regression is used in this paper [20]. The experiment was done several times and the data of rotation was taken to train the algorithm. The model of the algorithm in this case was a hyper-plane in the sixth dimension. The algorithm would take the current position, the current speed, and four previous values of speed. The mathematical model of the algorithm was of the form:

$$y' = XW \tag{10}$$

Where y' is the predicted angle, X is the input vector, and W is the parameter vector [21]. The vector W was found by training the algorithm using 4200 data point, and the model was tested on 1800 data point. The criterion of training was minimum squared error which is in the form:

$$E = \sum (y'_i - y_i)^2 \tag{11}$$

$$E = \sum (XW - y_i)^2 \tag{12}$$

In order to find the minimum E , the equation is differentiated and equated to zero.

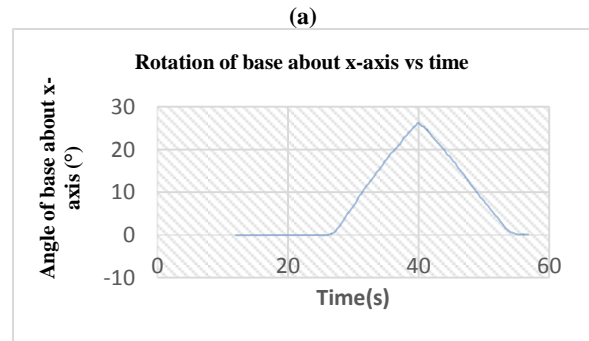
$$X'XW = X'y \tag{13}$$

$$W = (X'X)^{-1}X'y \tag{14}$$

Thus, the W calculated from (12) would yield the minimum squared error and is the one used in the prototype. Using the coefficient of determination (R^2) formula to test the algorithm:

$$R^2 = 1 - \frac{\sum (y'_i - y_i)^2}{\sum (y_{mean} - y_i)^2} \tag{15}$$

The coefficient of determination was about 0.998. When the system was analyzed with the linear regression algorithm, the vibration decreased from about 1° to about 0.5° and the maximum angle reached was about 1° (excluding the outlier) yielding a percentage error of about 4% compared to the previous 12% as shown in Figure 9.



(b)

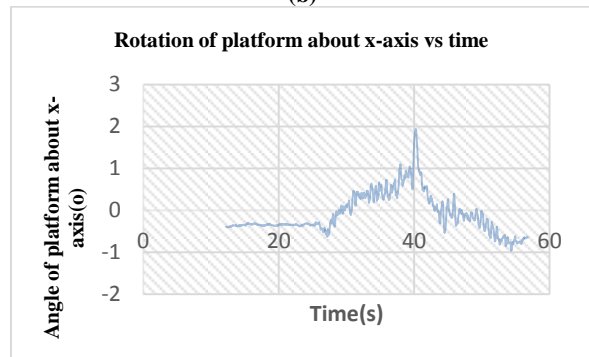


Figure 9. Rotation of (a) base and (b) platform w.r.t X-axis



6. CONCLUSION

The inverted 6-DOF parallel manipulator is utilized as vehicle stabilizer, where the upper platform orientation is designed to be stabilized at zero degrees at different base orientations due to variation in pathway elevations. Initially, the model was tested in Simulink environment to validate its capabilities to stabilize the system at practically large angles. The real prototype required more advanced controller to accommodate the nonparametric variables in real testing environment. In order to improve the controller, linear regression model was implemented to achieve more robust performance of the stabilizer. The maximum error reached decreased from 12% to about 4% and the level of vibration amplitude has decreased from about 1° to about 0.5° .

ACKNOWLEDGMENT

Authors gratefully acknowledge Abu Dhabi University for funding, support and help.

REFERENCES

- [1] L.W. Tsai, *Robotic Analysis: The Mechanics of Serial and Parallel Manipulators*, John-Wiley & Sons, New York, 1999.
- [2] J.P. Merlet, *Parallel robots (2nd ed.)*, Springer, France, 2006.
- [3] B. Dasgupta, and T.S. Mruthyunjaya, "The Stewart platform manipulator: A review," *Mechanism and Machine theory*, vol. 35, pp. 15-40, 2000.
- [4] E.F. Fitcher, "A Stewart Platform-Based Manipulator: General Theory and Practical Construction," *International Journal of Robotic Research*, vol. 5, no. 2, pp. 157-182, 1986.
- [5] J. P. Merlet, *Parallel Robots*, 2nd Edition, Sophia-Antipolis, France, Springer, 2006.
- [6] Z. Copeland, B. Jung, M. J. D. Hayes, and R. G. Langlois, "Atlas Motion Platform Full-Scale Prototype Design," *Recent Advances in Mechanism Design for Robotics*, Springer, pp. 249-259, 2015.
- [7] Y. Jin, I.-M. Chen and G. Yang, "Kinematic Design of a 6-DOF Parallel Manipulator," *IEEE Transactions on Robotics*, vol. 22, no.3, pp.545-551, 2006.
- [8] D. J. Gonzalez and H. H. Asada, "Design and analysis of 6-dof triple scissor extender robots with applications in aircraft assembly," *IEEE Robotics and Automation Letters*, vol.2, no. 3, pp. 1420-1427, 2017.
- [9] I. Bayati, M. Belloli, D. Ferrari, F. Fossati, and H. Giberti, "Design of a 6-DoF robotic platform for wind tunnel tests of floating wind turbines". *Energy Procedia*, vol. 53, pp. 313-323, 2014.
- [10] S.-K. Song and D.-S. Kwon, "Six-degrees-of-freedom parallel mechanism for micro-positioning work". *United States Patent US6477912 B2*, 12 Nov 2002.
- [11] J. Yang, Z. Xu, Q. Wu, ... et al, "Dynamic modeling and control of a 6-DOF micro-vibration simulator," *Mechanism and Machine Theory*, vol. 104, pp. 350-369, 2016.
- [12] S. Lee, J. Song, W. Choi, and D. Hong, "Position control of a Stewart platform using inverse dynamics control with approximate dynamics," *Mechatronics*, vol.13, pp.605-619, 2003.
- [13] T. Geike, and J. McPhee, "Inverse dynamic analysis of parallel manipulators with full Mobility," *Mechanism and Machine Theory*, vol. 38, pp. 549-562, 2003.
- [14] Z. Lazarevic, "Feasibility of a Stewart Platform with Fixed Actuators as a Platform for CABG Surgery Device," *Master's Thesis*, Columbia University, Department of Bioengineering, 1997.
- [15] Y. Lou, G. Liu, J. Xu, and Z. Li, "A general approach for optimal kinematic design of parallel manipulators," In *Proceedings of IEEE International Conference on Robotics and Automation*, New Orleans, LA, USA, pp. 3659-3664, 2004.
- [16] S. Pugazhenti, T. Nagarajan, and M. Singaperumal, "Optimal trajectory planning for a hexapod machine tool during contour machining," *Journal of Mechanical Engineering Science*, vol. 216, pp.1247-1257, 2002.
- [17] A. M. Mohammed and S. Li, "Dynamic Neural Networks for Kinematic Redundancy Resolution of Parallel Stewart Platforms," *IEEE Transactions on Cybernetics*, vol. 46, no. 7, pp. 1538-1550, 2015.
- [18] H. Tourajizadeh, M. Yousefzadeh, and A. Tajik, "Closed Loop Optimal Control of a Stewart Platform Using an Optimal Feedback Linearization Method," *International Journal of Advanced Robotic Systems*, vol.13, no. 3, pp. 134, 2016.
- [19] M. Becerra-Vargas and E. Belo, "Application of H Theory to a 6 DOF Flight Simulator Motion Base", *Journal of the Brazilian Society of Mechanical Sciences and Engineering* ,vol. 34, no.2, pp.193-204, 2012.
- [20] D. J. Olive, *Linear Regression*, Springer, 2017.
- [21] X. Yan, and X. G.Su, "Linear regression analysis: theory and computing," *International Statistical Review* ,vol. 78, no. 1, pp. 144, 2010.



Mohammad Alkhedher Associate Professor, Abu Dhabi University, has more than 12 years of academic experience, received his PhD in mechanical Engineering from Washington State University, USA in 2007. He has published about 40 Journal and conference papers. His research interest are in areas of Mechatronics, modeling, simulation and control of dynamic systems and Nanotechnology. He joined the Mechanical engineering department at Abu Dhabi University in 2017.



Tariq M. Younes He received the bachelor and Master Degrees in Biotechnical and medical apparatus and systems Engineering from Tver State Technical University 1998, and Ph.D degree in Instrumentation and measurement from Moscow State University of Environmental Engineering in 2004. In 2004, he joined Al Balqa Applied University in 2005. Since September 2007, he has been with the Department of Mechatronics Engineering at the same university, where he was an Assistant Professor, and became an Associate Professor in 2012.



Omar Mohamad has received his BSc. Degree in Mechanical engineering from Abu Dhabi University in 2018, currently pursuing his Master degree in Mechanical Engineering at the same university. He is a full time teaching assistant at the Mechanical Engineering

department. His research interests are in solid mechanics and robotics.



Uzair Ali has received his BSc. Degree in Mechanical engineering from Abu Dhabi University in 2018, currently pursuing his Master degree in Mechanical Engineering at the same university. He is a full time research assistant at the Mechanical Engineering department. His research interests are in solid mechanics and

robotics.